Review of Hybrid Multilevel Converter Topologies Utilizing Thyristors for HVDC Applications

Panagiotis Bakas, *Member, IEEE*, Yuhei Okazaki, *Member, IEEE*, Anshuman Shukla, *Senior Member, IEEE*, Siba Kumar Patro, *Student Member, IEEE*, Kalle Ilves, *Member, IEEE*, Frans Dijkhuizen, *Member, IEEE*, and Alireza Nami, *Senior Member, IEEE*

***Abstract*—Hybrid multilevel converters using bidirectional thyristors and IGBTs have gained significant interest in recent times, as they possess important features of both voltage-source and line-commutated converter technologies. This article presents a classification of hybrid multilevel converters for HVdc applications. The methodologies to derive, evaluate, and select these converter topologies are proposed as well. The hybrid converters are classified from the power device to the system configuration based on the analogy of the voltage-source converter and the current-source converter. Derivation methods of hybrid cell, cluster, arm, phase, and converter, based on the topology tree presented in this article, are applied to derive both existing and new hybrid converters. Comparisons show that hybrid converters have functionality similar to either the modular multilevel converter or the line-commutated converter, depending on the ratio between thyristor and active switch IGBT counts employed. Several hybrid-station configurations are discussed in order to suggest the most suitable converter topology for each configuration. The presented analysis can provide a point of reference and a useful framework for the future developments of hybrid multilevel converters for HVdc applications.**

***Index Terms*—DC–AC power conversion, HVdc transmission, hybrid converter, hybrid station, multilevel converters, thyristors.**

I. Introduction

HVDC transmission systems are increasing their accumulated installed power worldwide after the introduction of voltage-source-converter-based HVdc (VSC-HVdc) systems. The VSC-HVdc system opens up active research and development in both academia and industries. This has led to the commercially available VSC-HVdc systems up to 5 GW and ±800 kV today [5].

Manuscript received December 2, 2019; revised March 28, 2020; accepted May 14, 2020. Date of publication May 26, 2020; date of current version September 4, 2020. Recommended for publication by Associate Editor Z. Li. *(Corresponding author: Panagiotis Bakas.)*

Panagiotis Bakas, Yuhei Okazaki, Kalle Ilves, Frans Dijkhuizen, and Alireza Nami are with the ABB Power Grids Research, 721 78 Västerås, Sweden (e-mail: panagiotis.bakas@se.abb.com; yuhei.okazaki@se.abb.com; kalle.ilves@se.abb.com; frans.r.dijkhuizen@se.abb.com; alireza.nami@se.abb.com).

Anshuman Shukla and Siba Kumar Patro are with the Indian Institute of Technology Bombay, Mumbai 400076, India (e-mail: ashukla@ee.iitb.ac.in; sibakumarpatro@gmail.com).

Color versions of one or more of the figures in this article are available online at https://ieeexplore.ieee.org.

Digital Object Identifier 10.1109/TPEL.2020.2997961

HVdc systems based on the line-commutated converter (LCC) have been employed for bulk power transmission system. Currently available LCC-based HVdc systems feature power transmission capability up to 10 GW and 1100 kV[6]. Increasing electricity demands in, e.g., urban areas require stable power supply from remote locations with the lowest transmission losses, which brings an opportunity for high-power long-distance HVdc systems. The LCC-based HVdc systems have some limitations, such as the lack of reactive power control or black start capability, and have high reactive power consumption. On the other hand, the VSC-based HVdc system provides new functionalities (e.g., as summarized in [7]) complementing the LCC-based HVdc system as continuous reactive and active power control, power reversal with constant dc voltage polarity making dc multiterminal networks easier to implement.

Fig. 1 shows the evolution of the HVdc converter technology. The HVdc converter started back in 1972 with the first commercial application of the thyristor-based LCC technology. The progress of the semiconductor power device technology led to the high-voltage-insulated gate bipolar transistor (IGBT), which enabled the development of the two-level VSC technology. The first commercial installation of this technology was finalized in 1999. Furthermore, the VSC technology evolved by adopting the three-level VSC topology in 2000 to achieve better ac harmonic performance and higher conversion efficiency. The two-level and three-level VSCs are classified into the topology category of *monolithic converters* in [8]; this is because these converters consist of switches or VSC valves that are constructed as a single unit and are not modular. However, the achievable voltage and power levels from the two-level or three-level converter were far lower that of the LCC due to the current capability of the IGBTs. After the emergence of the modular multilevel converter (MMC) in 2003 from an academic paper [9], the MMC-based HVdc has been widely accepted in industry and has been commercially deployed for the first time in 2010. In contrast to the monolithic converters, the MMC is classified into the topology category of *modular converters* in [8]; this is because the MMC consists of submodules (SMs) that are simply connected in series to construct six modular VSC valves. The MMC, or modular converters in general, can provide high direct voltage while keeping high conversion efficiency due to its scalable converter structure. However, the MMC is only scalable for the voltage but not for the current. Therefore, the power capability of the

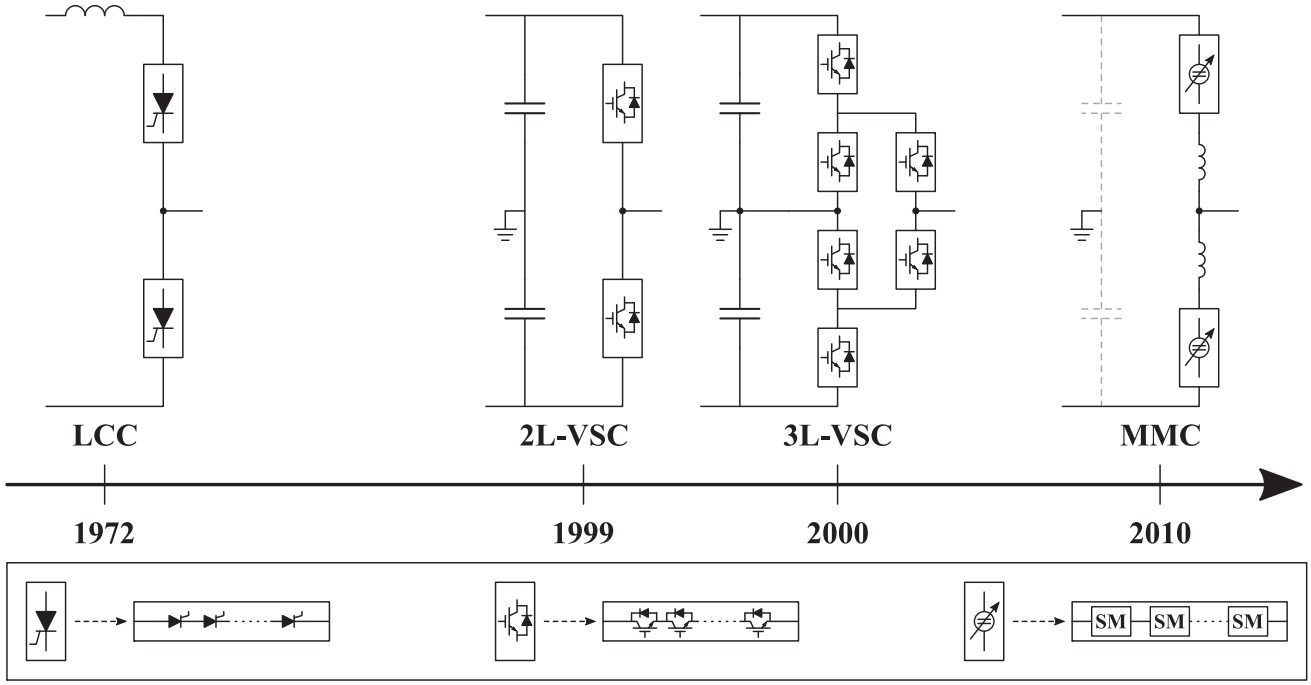

Fig. 1. Evolution of HVdc converter technology over time. The years mark the first commercial installation of each technology, namely: (1972) Eel River back-to-back LCC HVdc [1]; (1999) Gotland two-level VSC HVdc link [2], [3]; (2000) Eagle Pass back-to-back three-level VSC HVdc [3]; (2010) Trans Bay Cable MMC HVdc link [4].

MMC is the same as the monolithic converter under the same dc-link voltage.

A combination of two different power devices, notably IGBTs and thyristors, was investigated in [10] to achieve forced turn OFF of the bidirectional thyristors (i.e., two thyristors connected in antiparallel) by the help of IGBTs. The complicated switching sequence and control was one of the obstacles for the practical use of the topology discussed in [10]. However, the introduction of modular converters consisting of VSC SMs opened new possibilities in the implementation of forced thyristor turn OFF. Thus, the combination of thyristors and VSC SMs has recently gained more attention in the literature and it is the main topic of this article. Note that the converters formed by the combination of thyristors and VSC SMs and/or IGBTs are termed *hybrid converter* in this article.

Several hybrid converters have been proposed to reduce the number of required power devices from the MMC along with the capacitive energy reduction. Many of these hybrid converters have been derived from hybrid VSCs, which combine VSC SMs with monolithic VSC valves consisting of series-connected IGBTs. The hybrid converters are derived by replacing the monolithic VSC valves of the hybrid VSCs with thyristor-based valves. The first example of such hybrid VSC is the alternate arm converter (AAC) proposed in [11]–[14]. The series-connected SM counts of the AAC are reduced by replacing a part of the SMs of the MMC with a monolithic VSC valve constructed by series-connected power devices. The AAC generates inherent dc-link current ripple that can be taken care by either introducing a dc-link capacitor [15] or operating the converter with extended overlap time, as shown in [16] that describes the extended-overlap AAC (EO-AAC). The AAC with monolithic thyristor valves has been recently described in [17]. Moreover, the controlled-transition bridge (CTB) proposed in [18]–[20] requires lower number of semiconductor devices and capacitors. Another converter that has been proposed with both monolithic VSC valves and monolithic thyristor valves is the modular embedded multilevel converter (MEMC) described in [21]–[23]. The MEMC can reduce the number of required VSC SMs to half compared to the MMC. A proper control method can eliminate the harmonics on both dc and ac sides. Furthermore, the modular embedded thyristor-directed converter METDC has been proposed recently in [24] and it is similar to the series hybrid VSC presented in [25] and [26]. The METDC is derived from the series converter configuration that interconnects three single-phase converters in series (at the dc side). This series interconnection reduces the required blocking voltage of each modular VSC valve; thus, the series converter configuration offers a potential reduction of the required number of power devices.

In summary, most of the research in hybrid topology aims at reducing the number of required power devices and the capacitor requirements from the MMC. However, the reduced power-device count and the reduced capacitive energy requirement bring a consequence to the converter performance, such as dc/ac voltage/current coupling, dc/ac harmonics, and increased current rating of the IGBTs. Therefore, it is important to classify the hybrid topologies based on their structure and main performance characteristics.

This article provides a derivation method, evaluation method, and topology-selection method of the hybrid converters based

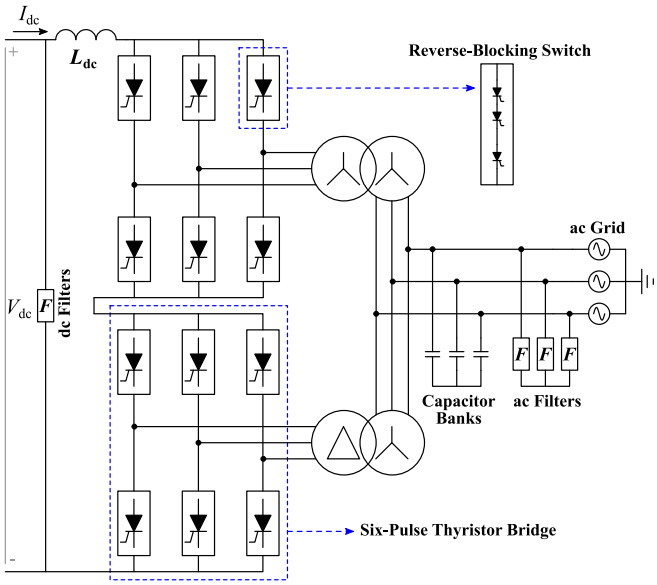

Fig. 2. 12-pulse LCC-HVdc station circuit schematic.

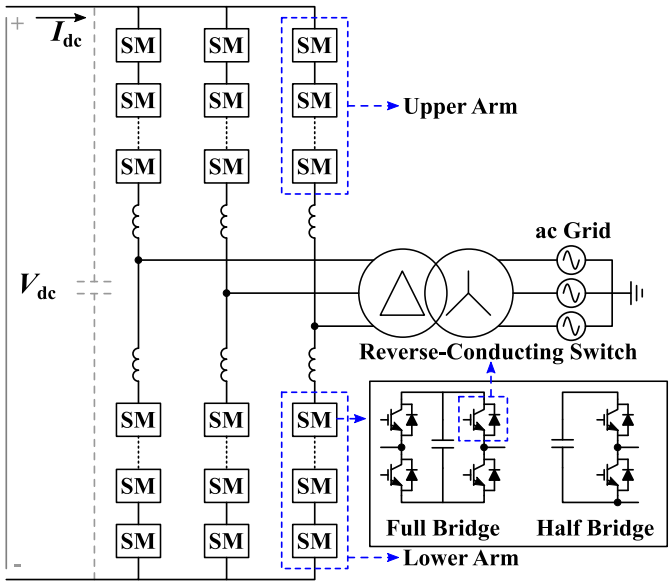

Fig. 3. MMC-HVdc station circuit schematic.

on the topology tree proposed in [8]. The state-of-the art hybrid converters proposed in the literature along with new converters are classified based on the topology tree. A qualitative and quantitative evaluation of various hybrid converters show that the combined power rating of VSC valves and thyristors indicates whether the hybrid converter has similar functionality to the LCC or the MMC. Furthermore, several hybrid-station configurations, where the LCC and a hybrid converter are connected either in series or parallel, are summarized to indicate criteria for selecting hybrid converter topologies that would allow both converters of the hybrid station to operate at their maximum power.

II. Characteristics and Comparisons of LCC and VSC Technologies for HVDC Transmission

A. LCC and MMC System Configurations for HVDC

The LCC HVdc technology facilitates bulk power transfer over long distances. The thyristors used in the LCC feature high reliability, robustness, low cost, and losses. They can block voltages of either polarity but conduct current only in one direction, which characterizes the current-source converter (CSC) operation. Hence, the power flow magnitude and direction in LCC are controlled by dc-link voltage control. Fig. 2 shows a typical LCC station consisting of mainly ac filters, shunt capacitor banks, converter transformers, dc reactors, dc filters, and dc lines or cables. The 12-pulse LCC is built by connecting two 6-pulse LCCs in series. Such arrangement improves the harmonic performance while increasing the power capability. The LCC also consumes the reactive power, which is supplied by the ac harmonic filters and the capacitor banks. The dc-link voltage of an n-pulse configuration contains harmonics of order $6n$ (n as a natural number) that are removed using dc filters and a dc reactor ($L_{\rm dc}$ in Fig. 2), which also limits the current and voltage transients.

The MMC-based HVdc system [9] offers added benefits such as modularity, scalability, low dc/ac filtering requirements, and high efficiency. Fig. 3 shows a circuit configuration of the MMC wherein each arm (also referred as *modular VSC valve*) consists of half- or full-bridge SMs (HB SMs or FB SMs) connected in series. This gives the freedom to connect as many SMs as required for achieving a certain harmonic performance, without increasing the circuit complexity. Each SM contains a dc capacitor, and several IGBTs with antiparallel diodes. Two arms are connected through suitably sized arm inductors. A three-phase MMC is formed by using six arms that share a common dc link, as shown in Fig. 3. Note that, even though the dc-link capacitors, depicted in dashed-gray line in Fig. 3, are not required for normal operation, they might be used in practice for grounding and/or protection purposes. Being a VSC, the dc-link voltage is held fixed and the power flow magnitude and direction are controlled by varying the current.

B. Comparison of LCC and MMC Systems

While the MMC offers more flexibility in control and enhanced operating performances, the LCC still has advantageous features such as higher power handling capability and lower losses among others. Some of their relevant merits, features, and limitations are summarized in Table I. In the MMC, a large number of SMs and their associated capacitors make the system costly and the capacitors are prone to failure too. Additional SMs are used to improve the reliability of MMC. Furthermore, the losses per unit of transferred power in an MMC are still higher than those of the LCC and the IGBTs used in the MMC cannot handle as high steady state and transient currents as the thyristors used in the LCC. Thus, the overall power and fault handling capabilities of the MMC are at much lower level than of LCC. Recently, the idea of using both thyristors and modular VSC valves in a single converter structure to construct a VSC

TABLE I
LCC-HVDC VERSUS MMC-HVDC COMPARISONS

Features	LCC	MMC
Semiconductors	Thyristors	IGBTs and antiparallel diodes
On-state (saturation) voltage/ rated voltage	0.2*	0.7*
Active power in bipolar configuration	12 GW with dc-link voltage of ±1100 kV [6]	5 GW with dc-link voltage of ±800 kV [5]
Independent control of active/reactive power	No	Yes
Black-start capability– Supplying passive networks	No	Yes
Sensitivity to ac grid disturbances	High	Low
Operation at low active power	No	Yes
DC-fault handling	Fault-current limiting possible	Fault-current limiting requires full-bridge or other bipolar SMs

*The thyristor ratio is calculated based on 8.5 kV, 3.7 kA phase-controlled thyristor [27] and the IGBT is calculated based on the 4.5 kV, 3 kA IGBT StakPak [28].

has gained significant research interests. The main objective of combining thyristors and modular VSC valves is to achieve the forced commutation of the thyristors, which enables increased conversion efficiency and dc-fault tolerance of the LCC besides retaining the VSC control flexibility. The following section describes this configuration in detail.

III. CLASSIFICATION OF HYBRID TOPOLOGIES

Fig. 4 shows the topology tree of the converters applicable to the HVdc system. The topology tree is an extended version of the one presented in [8]. The new family that is hybrid family is added in Fig. 4 along with a detailed classification of each component used in the converters. The hybrid topology layer is the combination of both VSC and CSC components. Note that the components referred here are described as switch, SM, cluster, arm, phase, converter, and station in Fig. 4. Each component is defined as follows.

1) *Switch:* Semiconductor power devices that has either reverse conducting (RC) and/or reverse blocking (RB) functionalities.
2) *Submodule (SM):* Fundamental building block of the circuit. The SM has two categories; one is monolithic block which does not have a capability of achieving power conversion by itself; the other is a VSC/CSC SM that can achieve the power conversion by itself as it comprises switches and energy storage components (capacitors and inductors).
3) *Cluster:* The connection of multiple SMs. The cluster can be either series connections of SMs or parallel connections of SMs.
4) *Arm:* One input one output system with dc and ac ports. It is equivalent to clustering all SMs in a single arm.
5) *Phase:* Two input ports and one output port system, where the two input side is dc and one output side is ac. It consists of two arms connected in series.
6) *Converter:* A system with two input ports and one output port, where the two port side is dc and three port side is ac. The converter comprises of three phases connected either in parallel or in series at the dc side.
7) *Pole/system:* Multiple connection of converters in either parallel or series.

The MMC and LCC explained in Section II can be derived by using the topology tree in Fig. 4. Attention should be paid to CSC-family category to derive LCC, whereas it should be paid to VSC-family category to derive the MMC. The LCC consists of RB switches connected in series to configure monolithic arm in the CSC-family category. Series connection of the monolithic arms becomes a CSC phase that leads to a final stage of configuring LCC by connecting three of the CSC phases in parallel. The MMC consists of VSC-SMs, i.e., half-bridge or full-bridge SMs, that are combination of *RC* switches and capacitors. Series connection of the VSC-SMs configures modular cluster and arm. Similarly to the LCC, series connection of the modular arms becomes a VSC phase that finally creates the MMC by connecting three of the VSC phases in parallel.

IV. DERIVATION OF HYBRID CONVERTERS

This section utilizes the topology tree shown in Fig. 4 to derive hybrid building blocks, which are employed in different configurations for constructing hybrid converters that combine thyristors and VSC elements.

At this point, it is important to highlight that the hybrid converters that utilize thyristors must overcome a common challenge; that is, controlling the thyristor turn-OFFprocess, as already described in [22], [23], [29]–[39]. Even though some hybrid converters can operate with natural thyristor turn OFF

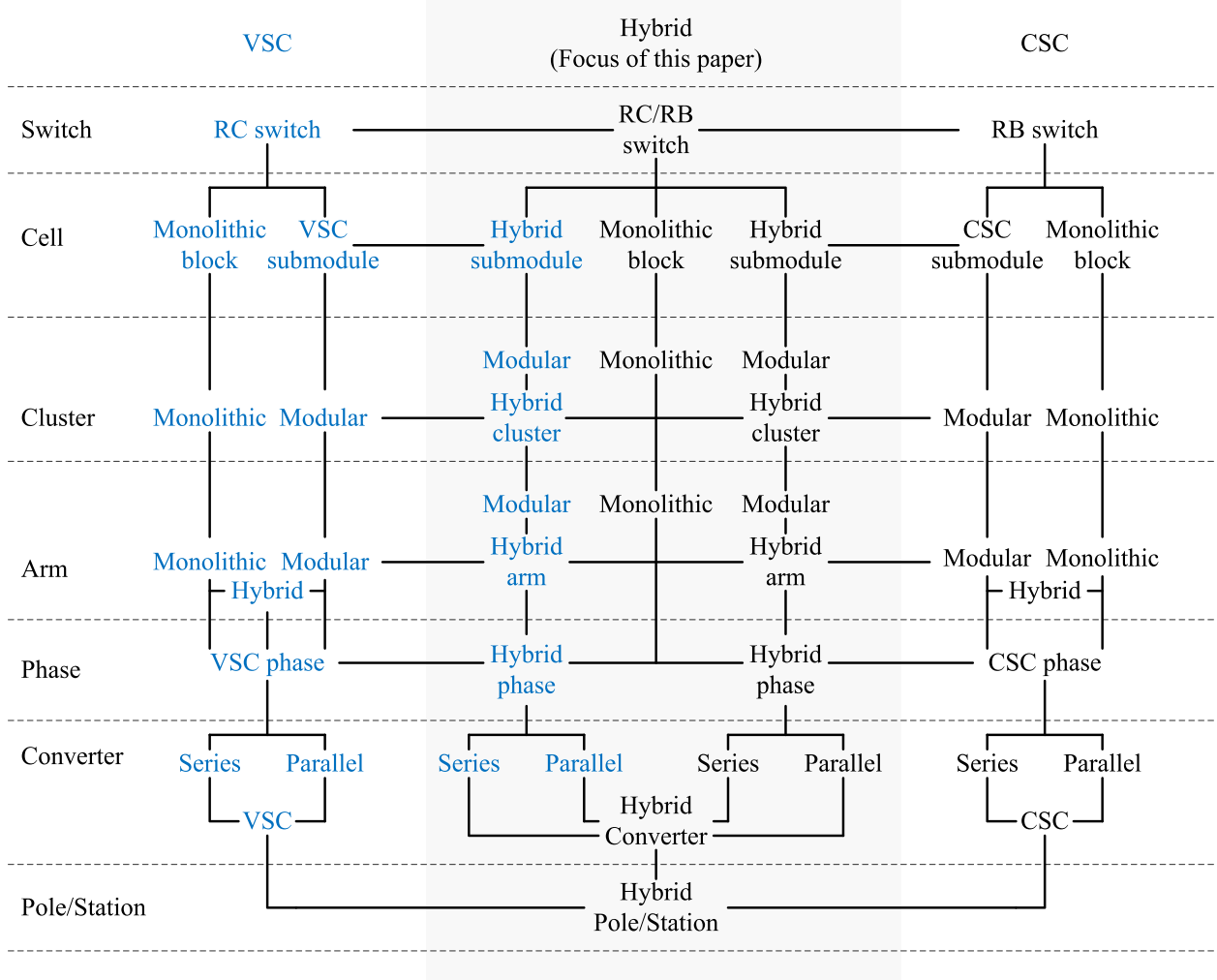

Fig. 4. Topology tree including hybrid topology family introduced in this article.

(i.e., turn OFF at zero-crossings of the thyristor current), the controllability of the hybrid converter is greatly enhanced by turning OFF the thyristors at nonzero current. The controllable turn OFF of the thyristors can be achieved by the VSC elements of the hybrid converters, provided that the following requirements are fulfilled.

1) When a conducting thyristor must be turned OFF, the VSC elements that are connected with the thyristor (either in series or in parallel) must inject a voltage that would drive the thyristor current to zero (or commutating the thyristor current to an alternative path).
2) The rate of change of thyristor current must not exceed the thyristor limit, which is typically in the range of $di/dt = 10$ A/μs for conventional thyristors.
3) Once the thyristor current becomes zero, the suitable VSC elements must keep the thyristor reversely biased for a certain time interval, which must be longer than the thyristor hold-OFF time t_q. If the thyristor becomes forward-biased before the t_q time has elapsed, it will start conducting current without triggering its gate. Note that di/dt limitation mentioned previously is important for this step, as the di/dt impacts the t_q time. Notably, increased di/dt rates lead to increased t_q times.
4) Once the t_q time has elapsed, the thyristor can be forward-biased without the risk of reconduction. Yet, the forward voltage must be applied at a limited dv/dt rate, in order to allow the thyristor to regain its forward-blocking capability and avoid the risk of accidental retriggering due to high dv/dt.
5) When a turned-OFF thyristors must be turned ON, the di/dt rate must again be limited to the specifications of the thyristor. Otherwise, there is a risk of uneven current distribution through the thyristor active area, which might lead to hot spots and finally thermal runaway of the active regions with the highest current densities.

A. *Hybrid Switch*

The most fundamental building block of the hybrid converters is the RC/RB switch, which is derived by combining RC or RB switches, as shown in Fig. 4. The RC and RB switches operate in two quadrants, as depicted in the left and right drawings of

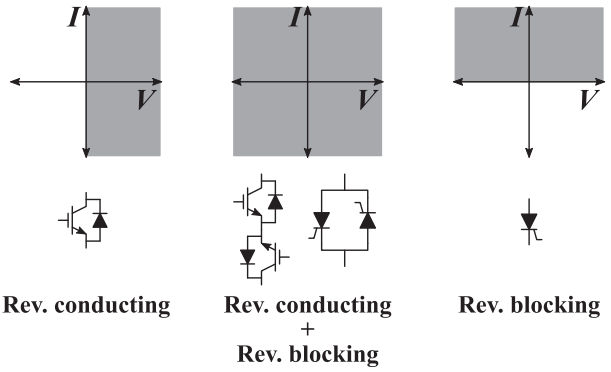

Fig. 5. Variations of switches and their corresponding quadrants of operation (gray areas): (left) IGBT-based RC switch; (right) thyristor-based RB switch; and (middle) IGBT- and thyristor-based RC/RB switches.

Fig. 5, respectively; that is, the RC switch conducts current in both directions but blocks voltage in one polarity, while the RB switch conducts current in one direction but blocks voltage in both polarities. The RC/RB switch, shown in the middle drawing of Fig. 5, can be constructed by the antiseries connection of two RC switches or by the antiparallel connection of two RB switches. As a result, the hybrid switch is capable of operating in all four quadrants; that is it can conduct current in both directions and block voltage in both polarities. As this article deals mainly with thyristor-based hybrid switches, the terms thyristor switch or valve are used instead of hybrid switch for clarity.

B. Hybrid SMs

As mentioned previously and depicted in Fig. 4, the hybrid SMs comprise of a combination of RC/RB switches and VSC or CSC SMs. In this way, a hybrid SM is an independent unit that can achieve power conversion by itself. Examples of hybrid SMs that are constructed by several RC/RB switches and a VSC SM are depicted in Fig. 6. As shown in Fig. 6, the SMs are connected either in series or parallel to the thyristors, in order to achieve forced commutation of the thyristors.

The one shown in Fig. 6(a) is termed hybrid T-type SM in this article, and is basically a thyristor-based half-bridge SM with a VSC SM connected between the midpoint of the capacitors and the midpoint of the RC/RB switches (thyristors). This hybrid SM can be considered as a special case of the AFCB, which was proposed in [29] and [30]. The main role of the VSC SM is to enable the forced-commutation of the thyristors by injecting the appropriate voltage for transferring the current from one thyristor switch to the other and for reverse-biasing the outgoing thyristor for the required t_{q} time. For this purpose, the voltage rating of the VSC SM needs to be higher than half of the rated voltage of the hybrid T-type SM. The current rating of the VSC SM should be roughly equal to that of the thyristors, but its RMS current should be fairly small if the VSC SM is utilized only during commutations.

The hybrid SM shown in Fig. 6(b) is similar to the one in Fig. 6(a) but with the FB SM, which is used as the commutation circuit, is now in series to the dc-link capacitor. This implies

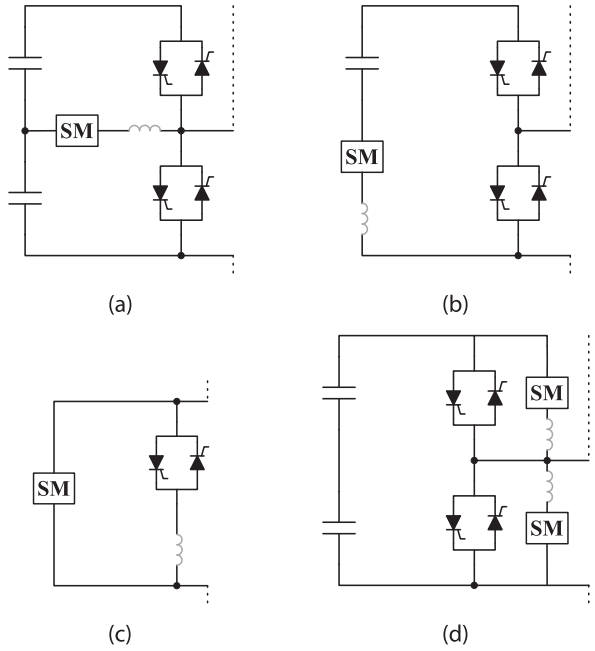

Fig. 6. Examples of hybrid SMs constructed by combining RC/RB switches and VSC SMs. (a) Active-forced commutated bridge (AFCB) [29], [30]. (b) Thyristor-based half bridge with semi-active capacitor. (c) Thyristor-based power SM (TBPG [31], [32], [37] with a single VSC SM). (d) Double commutation SM (DCSM) [38].

that the commutation circuit is in the main current path when this hybrid SM is inserted; thus, conduction losses are higher than the hybrid T-type SM, even though the voltage rating of the commutation circuit should be similar to the hybrid T-type SM.

The hybrid SM shown in Fig. 6(c) comprises a hybrid thyristor-based switch in parallel with a VSC SM. This hybrid SM can be considered as a special case of the thyristor-based power group (TBPG), which was proposed in [31], [32],[37], and [40], with only a single VSC SM and an RC thyristor switch; hence, it is termed thyristor-based power SM. The turn OFFof the thyristor switches is achieved by diverting the current through the VSC SM. When the thyristor current has been driven to zero, the VSC SM maintains a reverse voltage across the outgoing thyristor for the required t_{q} time, so that the thyristor turns OFF successfully.

For all the previous hybrid SMs the commutation circuit, i.e., the VSC SM, needs to conduct the full thyristor current for short period of time. The IGBTs used in the VSC SM experience high peak current but low RMS current. This is not the case for the hybrid SM of Fig. 6(d) due to the presence of two VSC SMs [38]; thus, this hybrid SM is termed DCSM. These VSC SMs act as the commutation circuit and can share the thyristor current during the commutation; thus, the peak current rating of the VSC SMs can be lower than that of the thyristors. Alternatively, it is possible to use only one VSC SM as the commutation circuit, provided that the VSC SM has the same current rating as the thyristor. This variation of the hybrid SM of Fig. 6(d) was proposed and presented in [41].

All of these hybrid SMs can be utilized in a modular converter configuration (i.e., as for the MMC shown in Fig. 3), in the same

manner as the SMs of the MMC. Moreover, the utilization of the thyristors as main switches increases the efficiency and the current capability of the hybrid SMs compared to the equivalent SMs of an MMC. The higher current capability of the thyristors could be utilized for handling faults, such as a dc fault. In such case, the antiparallel thyristors that form the hybrid SM bypass path can be triggered to isolate the ac and dc sides of the MMC with the hybrid SMs, in a similar manner as in [42]. In addition, the thyristor switches offer crowbar functionality for the hybrid SM of Fig. 6(a) to protect the SM from explosion, similarly to the one described in [43].

The main downside of all hybrid SMs is that the controllability of the output voltage is lost during the turn-OFF process of the thyristors due to the commutation time. This is because the VSC SM in any of these hybrid SMs is occupied with commutating the thyristor current and ensuring that the latter remains reverse-biased for the t_{q} time. Therefore, the output voltage of the hybrid SM during the commutation process is strictly defined by the requirements of the thyristor turn-OFF process. Moreover, the commutation voltage impacts the quality of the converter output voltage, if left uncompensated. Thus, additional hybrid SMs might be required in the converter arm for compensating the commutation voltage, which directly influence the redundancy requirements.

C. Hybrid Cluster/Arm

The hybrid cluster is another building block that can be used for constructing hybrid converters. As mentioned previously and depicted in Fig. 4, the hybrid cluster can be a combination of hybrid SMs, as well as a combination of monolithic RC/RB switches with modular clusters of VSC or CSC SMs. Three examples of hybrid clusters are depicted in Fig. 7(a)–(c). The hybrid cluster shown in Fig. 7(a) was proposed in [29] and [30] and is basically an HB SM constructed with monolithic RC/RB switches, complemented with a modular cluster of VSC SMs that is employed for enabling the forced commutation of the RC/RB switches. This cluster, proposed in [29] and [30], is termed AFCB cluster and its structure is similar to that of the AFCB hybrid SM shown in Fig. 6(a).

The second cluster, depicted in Fig. 7(b) and proposed in [31]–[33], [37], and [40], has similar structure to the TBPG SM shown in Fig. 6(c); thus it is termed TBPG cluster. The TBPG cluster consists of a modular cluster of VSC SMs (either FB SMs, as proposed in [37], [31], [40], and [32], or a combination of FB and HB SMs, as proposed in [33]) that is connected in parallel to a monolithic RC/RB switch. This RC/RB switch is used for bypassing the VSC cluster, while the latter is employed for enabling the forced commutation of the RC/RB switch.

The cluster shown in Fig. 7(b) can be further used to realize the thyristor-based HB cluster shown in Fig. 7(c). This cluster is termed DCCL cluster, as it has similar structure to the DCSM shown in Fig. 6(d) and proposed in [38]. In the DCCL cluster, two TBPG clusters are used along with a high voltage capacitor or several capacitors connected in series to support high voltage. Each TBPG of the DCCL cluster, which is constructed by two antiparallel thyristors connected in parallel to a cluster of VSC

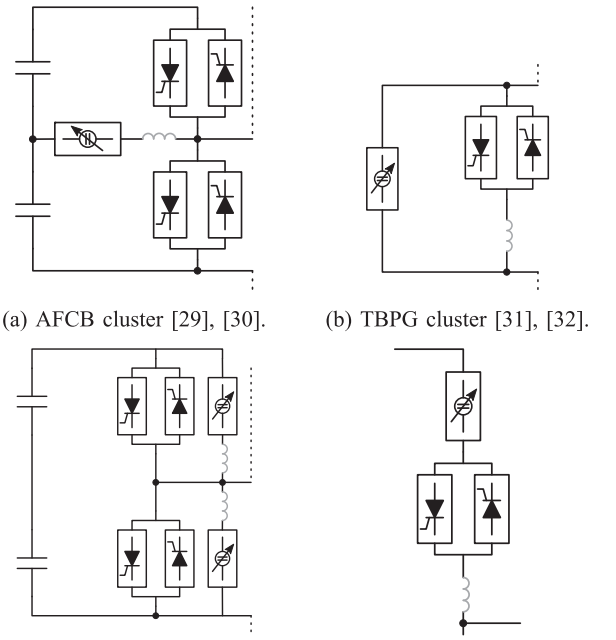

(a) AFCB cluster [29], [30]. (b) TBPG cluster [31], [32].

(c) DCCL cluster [38]. (d) TH-AAC arm [17], [39], [44].

Fig. 7. Example of (a)–(c) hybrid clusters constructed by combining monolithic RC/RB switches and modular clusters of VSC SMs, and of (d) a hybrid arm constructed by combining monolithic RC/RB switches and a modular arm of VSC SMs. (a) AFCB cluster [29], [30]. (b) TBPG cluster [31], [32]. (c) DCCL cluster [38]. (d) TH-AAC arm [17], [39], [44].

SMs, can be operated in the same way as described previously for the TBPG cluster of Fig. 7(b). The ac-terminal voltage of the DCCL cluster is equal to the capacitor voltage if the current flows through the thyristors of the upper TBPG cluster. Conversely, the ac-terminal voltage of the DCCL cluster is equal to zero if the current flows through the thyristors of the lower TBPG cluster.

In a similar manner, a hybrid arm can be constructed by the combination of monolithic RC/RB switches with modular arms of VSC or CSC SMs, or by the series connection of several hybrid clusters. Since this article focuses on hybrid clusters and arms based on VSC SMs, only VSC-based hybrid clusters and arms are discussed. An example of a hybrid arm, which has been proposed in [17], [39], and [44], is presented in Fig. 7(d), where a modular arm of VSC SMs is connected in series with series-connected thyristors. In this case the VSC arm is responsible for controlling the current through the RC/RB switch, as well as for forward- or reverse-biasing the RC/RB switch. For achieving both of these purposes, the VSC arm should generate an appropriate voltage with respect to the voltage of the circuit components that are connected in parallel to the hybrid arm.

D. Hybrid Phase

The next building block for deriving hybrid converters is the hybrid phase, which is a combination of a monolithic phase constructed by RC/RB switches with a modular VSC phase, as illustrated in Fig. 4. Four examples of hybrid phases are illustrated in Fig. 8. The hybrid phase shown in Fig. 8(a) resembles in structure the hybrid cluster of Fig. 7(a), but it consists of

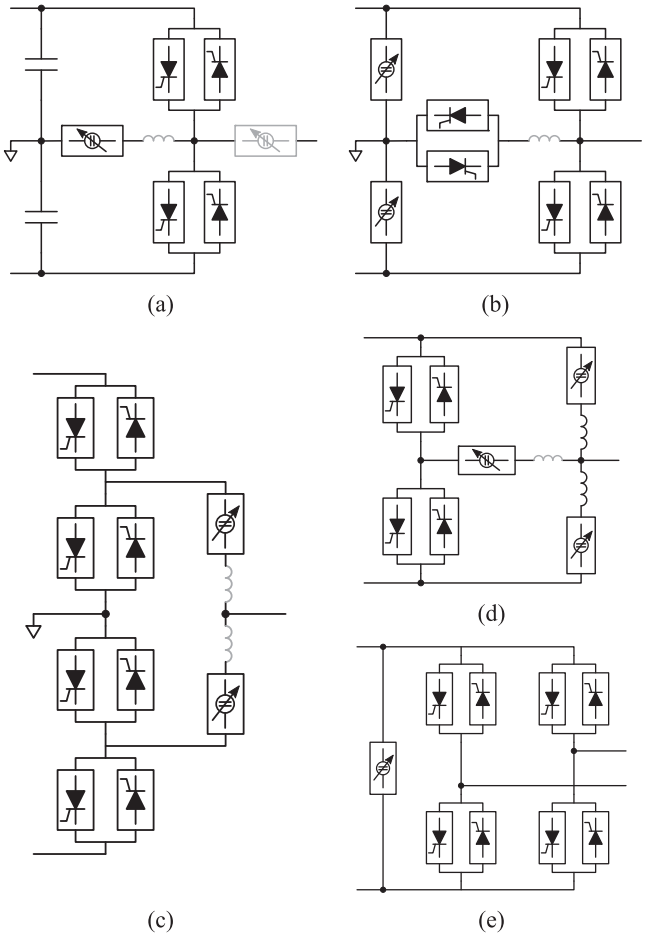

Fig. 8. Examples of hybrid phases constructed by combining monolithic RC/RB switches and modular VSC arms/phases: (a) ECTB [34]; (b) TH-2LC [36]; (c) MEMC [21]–[23]; (d) HACC [45]; and (d) METDC [24] hybrid phases.

three terminals instead of two and it is used as a complete phase of a hybrid converter, as shown in [20] and [30]. However, the principle of operation is the same, as the modular phase of VSC SMs, which is connected between the midpoints of the capacitors and the RC/RB switches, is again employed for enabling the forced commutation of the RC/RB switches. Note that another modular VSC phase [gray symbol in Fig. 8(a)] can be connected to the terminal at the midpoint of the RC/RB switches for serving various purposes that are discussed in Section IV-E. As the hybrid phase of Fig. 8(a) is employed to construct the enhanced controlled-transition-bridge converter (ECTB) proposed in [34], it is termed ECTB phase.

The hybrid phase shown in Fig. 8(d) comprises a modular phase of two modular arms of VSC SMs, a monolithic phase of RC/RB switches, and an additional modular phase of VSC SMs. The latter is connected at the midpoint of the monolithic phase of RC/RB switches. Thus, this modular VSC phase is responsible for controlling the current through the RC/RB switches and enabling the forced commutation of the latter. This hybrid phase is employed to construct the hybrid alternate-common-arm converter (HACC) presented in [35] and [45]; hence, it is termed HACC phase.

Moreover, the hybrid phase shown in Fig. 8(b), proposed in [36], is constructed in a similar manner as the hybrid phase in Fig. 8(d), with the difference that the modular VSC phase connected at the midpoint of the monolithic phase of RC/RB switches is substituted by a monolithic phase of RC/RB switches. This hybrid phase is employed to construct the thyristor-based two-level converter (TH-2LC) presented in [36]; thus, it is termed TH-2LC phase.

Another hybrid phase that is constructed by combining a phase of monolithic RC/RB switches with a modular VSC phase is depicted in Fig. 8(c). In this case, the RC/RB switches are employed for reconfiguring the connection of the two terminals of the modular VSC phase with the other terminals of the hybrid phase. In turn, the modular VSC phase is responsible for controlling the current through the RC/RB switches and enabling their forced commutation. As the hybrid phase of Fig. 8(c) is employed to construct the MEMC proposed in [22] and [23], it is termed MEMC phase. Converters constructed by hybrid phases have been proposed recently in [46] and [47].

E. Derivation of Hybrid Converters

Hybrid converters can be derived by combining any of the hybrid components mentioned so far and constructed by the topology tree of Fig. 4. In order to further clarify the derivation of hybrid converters, the fundamental converter configurations are depicted in Fig. 9 and are summarized as follows.

1) Modular configuration is shown in Fig. 9(a): the basic building block of this configuration is the hybrid SM or the hybrid cluster (abbreviated as HC). Multiple building blocks are connected in series to construct an arm, two arms are interconnected to construct a phase, and three phases are interconnected to construct a converter.
2) Arm configuration shown in Fig. 9(b): the basic building block of this configuration is the hybrid arm. Two building blocks are interconnected to construct a phase, and three phases are interconnected to construct a converter.
3) Parallel-phase configuration shown in Fig. 9(c): the basic building block of this configuration is the hybrid phase. Three phases are interconnected to construct a converter.
4) Series-phase configuration shown in Fig. 9(d): the basic building block of this configuration is the hybrid phase. Three phases are interconnected in series on the dc side to construct a converter. Note that this configuration mandates the use of single-phase transformers for avoiding dc offsets to the ac side.

The derivation of hybrid converters based on the configurations of Fig. 9 is demonstrated by the examples presented in the following paragraphs.

Examples of using the modular configuration of hybrid clusters, shown in Fig. 9(a), are the AFCB-MMC proposed in [29] and [30] and the TBPG-MMC proposed in [31]–[33]. The AFCB-MMC and the TBPG-MMC can be derived by interconnecting the hybrid clusters of Fig. 7(a) and (b), respectively, in the modular configuration of Fig. 9(a). An example of using the arm configuration of Fig. 9(b) is the AAC with thyristors, which was proposed in [17],[39], and [44]. This converter can

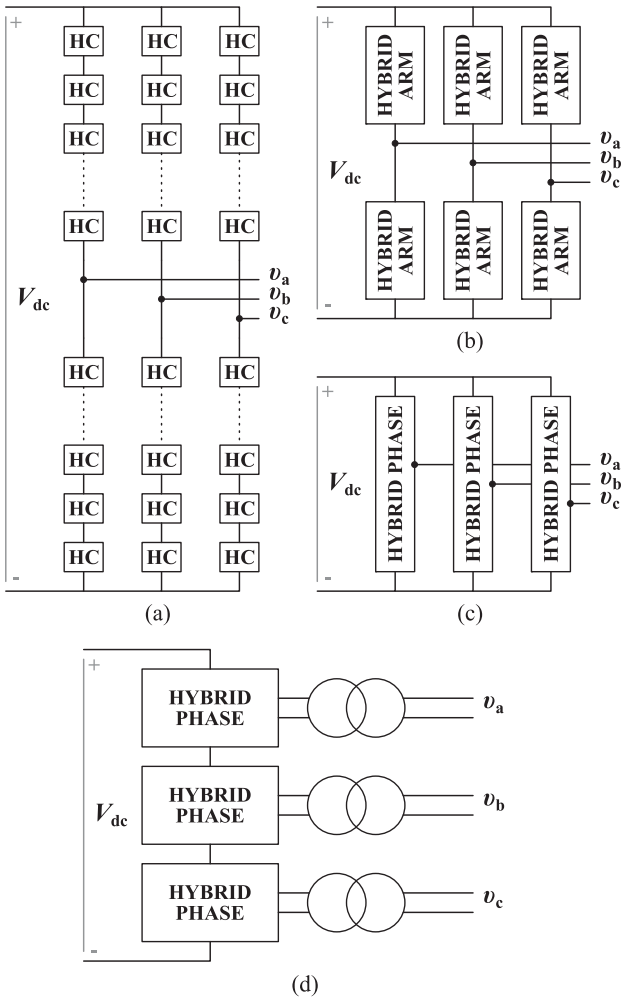

Fig. 9. Fundamental converter configurations: (a) modular (HC: Hybrid SM or Hybrid Cluster), (b) arm, (c) parallel-phase configuration, and (d) series-phase configuration.

be derived by connecting the hybrid arm of Fig. 7(d) in the arm configuration shown in Fig. 9(b).

Hybrid converters can also be constructed by combining hybrid phases in the configuration of Fig. 9(c). The parallel-phase converter constructed with the hybrid phase of Fig. 8(a) was proposed in [34] and is termed enhanced controlled-transition bridge (ECTB), as it is an enhanced version of the controlled-transition-bridge converter (CTB) proposed in [20]. The HACC proposed in [45] is another example of a hybrid converter constructed by employing the hybrid phase of Fig. 8(b) in the configuration of Fig. 9(c). The hybrid phase of Fig. 8(b) can be employed in the configuration of Fig. 9(c) in order to construct the TH-2LC proposed in [36]. Another hybrid converter that is constructed by hybrid phases is the MEMC, which is proposed in [22] and [23] and consists of three hybrid phases [as the one shown in Fig. 8(c)] interconnected in the configuration of Fig. 9(c). The hybrid phase of this converter is a combination of a modular VSC phase (with two modular VSC arms) with monolithic RC/RB switches that connect the former to the dc terminals.

The METDC, proposed in [24], is constructed by interconnecting the hybrid phase of Fig. 8(e) in the series configuration of Fig. 9(c); thus, the METDC belongs to the family of series-connected hybrid converters. Each phase of this hybrid converter contains monolithic RC/RB switches and a modular VSC phase, which comprises mainly HB SMs combined with a few FB SMs that are required for forced commutation purposes. The modular VSC phase is used to control the current through the RC/RB switches and for achieving forced commutation of the RC/RB switches, which are connected in an H-bridge configuration. Moreover, these modular VSC phases are used to support the dc link voltage, while the RC/RB switches of each hybrid phase are used to selectively connect the terminals of the corresponding modular VSC phase to the output ac terminals.

At this point, some considerations about the relation of the configurations of Fig. 9 should be provided. Notably, the arm configuration of Fig. 9(b) is related to the parallel-phase configurations of Fig. 9(c) in the sense that two hybrid arms can form a hybrid phase. Similarly, the modular configuration of Fig. 9(a) is related to the arm and parallel-phase configurations, as series-connected hybrid clusters/SMs can form a hybrid arm or a hybrid phase. Yet, it is important to clarify that the opposite relations do not hold, as a hybrid phase is not always modular and hence cannot be represented by a modular configuration. Moreover, employing the same building block in different configurations yield converter with different operational characteristics. For example, the AFCB cluster can be used in the modular configuration, leading to the AFCB-MMC proposed in [29], but also in the parallel-phase configuration, leading to a CTB structure with very different characteristics than the AFCB-MMC, as shown in [30]. Therefore, the selection of the configuration is closely related to the considered hybrid component.

In summary, this section described a derivation method of hybrid converters based on Fig. 9 and the hybrid converter components described in this section. This method can be utilized for deriving and classifying various hybrid converters that have been already proposed in the literature or for deriving new hybrid converters.

V. Assessment of Hybrid Converters

A. Comparison of Hybrid Converters

After the derivation of hybrid converter, it is important to distinguish either it is worth studied in detail or not based on its functionality. In this section, the hybrid converters that have been presented in Section IV-E (except for the TH-2LC because its ac and dc sides are strongly coupled and its modulation index range is very limited) are compared in a qualitative manner, based on the following criteria:

1) conduction losses of converter valves;
2) range of modulation indexes at which the converter can operate (coupling of ac and dc sides);
3) harmonic voltages/currents for ac/dc sides;
4) combined power rating per unit of transferred power of thyristors and VSC valves with respect to the FB-MMC.

Moreover, the conditions and assumptions employed for this comparison are listed as follows:

TABLE II
COMPARISON OF COMBINED POWER RATING OF SEMICONDUCTORS FOR ALL HYBRID CONVERTERS SHOWN IN SECTION IV-E WITH RESPECT TO THE FB-MMC

	FB-MMC	AFCB-MMC [29], [30]	TBPG-MMC [31], [32]	AAC [17], [44]	ECTB [34] {CTB [20]}	MEMC [22], [23]	HACC [35], [45]	METDC [24]
Building block (BB)	Fig. 3	Fig. 7(a)	Fig. 7(b)	Fig. 7(d)	Fig. 8(a)	Fig. 8(c)	Fig. 8(d)	Fig. 8(e)
Configuration of building blocks (BBs)	Fig. 9(a)	Fig. 9(a)	Fig. 9(a)	Fig. 9(b)	Fig. 9(c)	Fig. 9(c)	Fig. 9(c)	Fig. 9(d)
Number of BBs per phase ($N_{\mathrm{bb}}^{\mathrm{ph}}$)	$N_{\mathrm{bb}}^{\mathrm{ph}}$	$N_{\mathrm{bb}}^{\mathrm{ph}}$	$N_{\mathrm{bb}}^{\mathrm{ph}}$	2	1 {1}	1	1	1
Number of thyristor valves per BB ($N_{\mathrm{valve}}^{\mathrm{bb}}$)	–	2	1	1	2 {2}	4	2	4
Number of thyristors per valve (N_{dev})	–	2	2	2	2 {2}	2	2	2
Peak voltage of each thyristor valve ($V_{\mathrm{valve}}^{\mathrm{pk}}$)	–	$\frac{2V_{\mathrm{dc}}}{N_{\mathrm{bb}}^{\mathrm{ph}}}$	$\frac{2V_{\mathrm{dc}}}{N_{\mathrm{bb}}^{\mathrm{ph}}}$	$\frac{2V_{\mathrm{dc}}}{3}$	V_{dc} $\{V_{\mathrm{dc}}\}$	$\frac{V_{\mathrm{dc}}}{2}$	V_{dc}	$\frac{V_{\mathrm{dc}}}{2}$
Sum thyristor voltage rating per phase ($V_{\mathrm{valve}}^{\Sigma,\mathrm{ph}}$)	–	$8V_{\mathrm{dc}}$	$4V_{\mathrm{dc}}$	$\frac{8V_{\mathrm{dc}}}{3}$	$4V_{\mathrm{dc}}$ $\{4V_{\mathrm{dc}}\}$	$4V_{\mathrm{dc}}$	$4V_{\mathrm{dc}}$	$4V_{\mathrm{dc}}$
Peak current of each thyristor valve ($I_{\mathrm{valve}}^{\mathrm{pk}}$)	–	$\frac{3}{4}\hat{I}_{\mathrm{o}}$	$\hat{I}_{\mathrm{o}}$	$\hat{I}_{\mathrm{o}}$	$\hat{I}_{\mathrm{o}}$ $\{\hat{I}_{\mathrm{o}}\}$	$\frac{3}{4}\hat{I}_{\mathrm{o}}$	$\frac{3}{8}\hat{I}_{\mathrm{o}}$	$\hat{I}_{\mathrm{o}}$
Number of VSC valves per BB ($N_{\mathrm{valve}}^{\mathrm{bb}}$)	1	1	1	1	2 {1}	2	[2,1]*	1
Number of devices per VSC valve (N_{dev})	4	4	4	4	4 {4}	4	4	2†
Peak voltage of each VSC valve ($V_{\mathrm{valve}}^{\mathrm{pk}}$)	$\frac{2V_{\mathrm{dc}}}{N_{\mathrm{bb}}^{\mathrm{ph}}}$	$\frac{1}{2}\frac{2V_{\mathrm{dc}}}{N_{\mathrm{bb}}^{\mathrm{ph}}}$	$\frac{2V_{\mathrm{dc}}}{N_{\mathrm{bb}}^{\mathrm{ph}}}$	$\frac{2V_{\mathrm{dc}}}{3}$	$\frac{V_{\mathrm{dc}}}{2}$ $\left\{\frac{V_{\mathrm{dc}}}{2}\right\}$	$\frac{V_{\mathrm{dc}}}{2}$	$\left[V_{\mathrm{dc}}, \frac{V_{\mathrm{dc}}}{2}\right]$*	$\frac{V_{\mathrm{dc}}}{2}$
Sum VSC-valve voltage rating per phase ($V_{\mathrm{valve}}^{\Sigma,\mathrm{ph}}$)	$8V_{\mathrm{dc}}$	$4V_{\mathrm{dc}}$	$8V_{\mathrm{dc}}$	$\frac{16V_{\mathrm{dc}}}{3}$	$4V_{\mathrm{dc}}$ $\{2V_{\mathrm{dc}}\}$	$4V_{\mathrm{dc}}$	$10V_{\mathrm{dc}}$	V_{dc}
Peak current of each VSC valve ($I_{\mathrm{valve}}^{\mathrm{pk}}$)	$\frac{3}{4}\hat{I}_{\mathrm{o}}$	$\frac{3}{4}\hat{I}_{\mathrm{o}}$	$\hat{I}_{\mathrm{o}}$	$\hat{I}_{\mathrm{o}}$	$\hat{I}_{\mathrm{o}}$ $\{\hat{I}_{\mathrm{o}}\}$ ‡	$\frac{3}{4}\hat{I}_{\mathrm{o}}$	$\frac{3}{8}\hat{I}_{\mathrm{o}}$	$\hat{I}_{\mathrm{o}}$
Thyristor power rating (p.u. wrt FB-MMC)	–	1	0.67	0.44	0.67 {0.67}	0.5	0.25	0.67
VSC power rating (p.u. wrt FB-MMC)	1	0.5	1.33	0.89	0.67 {0.33}	0.5	0.63	0.17

The combined power rating was calculated for the same transferred power, dc-link voltage V_{dc}, modulation index $M=1$ and power factor $\cos\phi=1$. Note that $\hat{I}_{\mathrm{o}}$ represents the amplitude of the ac-side current.

*Note that the two-element vector notation, i.e., [x,y], denotes that the corresponding component is used in two different parts of the converter circuit that require different ratings. Thus, the semiconductor power rating of the corresponding component is calculated in two steps: (a) element-wise multiplication of the associated two-element vectors and multiplication with the scalar values, as specified by (1); (b) summation of the results of the element-wise calculations performed in step (a).

†The VSC valves of the METDC comprise only a small number of FB SMs that are required for the forced commutation of the thyristor valves. Hence, for the rating calculations it is assumed that the METDC's VSC valves consist only of HB SMs; so the number of devices is set to $N_{\mathrm{dev}}=2$ that represents HB SMs.

‡This represents a worst case, as the peak current of the VSC valves for the ECTB and the CTB might be lower than $\hat{I}_{\mathrm{o}}$, depending on the thyristor-commutation instants.

1) the conduction losses have been evaluated based on the type and number of components that are in the main current path;
2) the modulation index range has been defined as wide/narrow/tight depending on whether the converter can regulate the ac-side voltage in a wide/narrow range, respectively, but without affecting the dc-side voltage—this is termed also as ac-/dc-side coupling;
3) harmonic voltages/currents for ac/dc sides have been only qualitatively evaluated, based on the operating principles of the converter and not via detailed studies or simulations (alternatively, if simulation/experimental results have been presented in the related papers, the harmonics have been evaluated from these results);
4) the thyristor-based AAC was assumed to operate in a similar manner as the EO-AAC described in [16], i.e., with wide modulation index range and without sixth-order harmonic in the dc-link voltage;
5) the combined power rating per unit of transferred power is the ratio of the combined power rating of semiconductor devices and the power transferred by the converter;
6) the reference (i.e., 1 p.u.) for the relative per unit calculations is the combined power rating of the VSC clusters of the FB-MMC;
7) the calculation of the combined power rating of thyristors and VSC valves has been performed for the same transferred power, dc-link voltage, modulation index $M=1$, and power factor $\cos\varphi=1$.

The combined power rating is calculated as the product of the blocking voltage, the peak current, the number of devices per valve, and the number of valves per converter, where valve stands for either a thyristor valve or a VSC arm/cluster; notably, the combined power rating is given by

$$S_{\mathrm{valve}} = 3N_{\mathrm{bb}}^{\mathrm{ph}} N_{\mathrm{valve}}^{\mathrm{bb}} N_{\mathrm{dev}} V_{\mathrm{valve}}^{\mathrm{pk}} I_{\mathrm{valve}}^{\mathrm{pk}} = 3V_{\mathrm{valve}}^{\Sigma,\mathrm{ph}} I_{\mathrm{valve}}^{\mathrm{pk}} \quad (1)$$

where S_{valve} is the combined power rating of the valves in VA, $N_{\mathrm{bb}}^{\mathrm{ph}}$ is the number of building blocks per phase, $N_{\mathrm{valve}}^{\mathrm{bb}}$ is the number of valves per building block, N_{dev} is the number of semiconductor devices for the main component of the valve, $V_{\mathrm{valve}}^{\mathrm{pk}}$ and $I_{\mathrm{valve}}^{\mathrm{pk}}$ the blocking voltage in V and peak current in A of each valve. Note that the product of $N_{\mathrm{bb}}^{\mathrm{ph}}$, $N_{\mathrm{valve}}^{\mathrm{bb}}$,

TABLE III
QUALITATIVE COMPARISON OF HYBRID CONVERTERS SHOWN IN SECTION IV-E WITH RESPECT TO THE FB-MMC

	FB-MMC	AFCB-MMC [29], [30]	TBPG-MMC [31], [32]	AAC [17], [44]	ECTB [34] {CTB [20]}	MEMC [22], [23]	HACC [35], [45]	METDC [24]
Conduction losses of converter valves	High	Low	Low	Medium	Medium {Low}	Medium	High	Low
Modulation index range (ac/dc-side coupling)	Wide (No)	Wide (No)	Wide (No)	Wide (No)	Wide (No) {Narrow (Yes)}	Wide (No)	Narrow (No)	Narrow (Yes)
Low-order voltage harmonics (ac/dc side)	Low/Low	Medium/Low	Low/Low	Low/Low	Low/Low {High/Low}	Low/Low	Low/Low	Low/Medium
Low-order current harmonics (ac/dc side)	Low/Low	Medium/Low	Low/Low	Low/Low	Low/Low {High/Low}	Low/Low	Low/Low	Low/Medium
STATCOM operation during dc faults	Yes	No	Yes	Yes	Yes {Yes}	Yes	Yes	No

Note that all hybrid converters feature dc-fault ride-through capability. Regarding the modulation index range, the denotations *narrow* and *wide* imply capability to vary the modulation index by $<\pm 20\%$ and $>\pm 20\%$ from the nominal value, respectively.

N_{dev}, and $V_{\mathrm{valve}}^{\mathrm{pk}}$ yields the sum voltage rating of the valve per phase, which is represented by $V_{\mathrm{valve}}^{\Sigma,\mathrm{pk}}$ in (1). In order to clarify some of the aforementioned variables, the FB-MMC is used as example. More specifically, the FB-MMC is considered to be constructed by combining $N_{\mathrm{bb}}^{\mathrm{ph}}$ building blocks (i.e., FB SMs) per phase, while each VSC valve comprises a single building block (in this case the VSC valve is the same as the VSC SM), i.e., $N_{\mathrm{valve}}^{\mathrm{bb}}=1$. Thus, $N_{\mathrm{dev}}=4$, as the main component of the VSC valve is the FB SM that comprises four IGBT devices.

Then, the normalized combined power rating of each hybrid converter is calculated by

$$S_{\mathrm{norm}}^{\mathrm{hyb}}=\frac{S_{\mathrm{valve}}^{\mathrm{hyb}}/S_{\mathrm{o}}^{\mathrm{hyb}}}{S_{\mathrm{valve}}^{\mathrm{MMC}}/S_{\mathrm{o}}^{\mathrm{MMC}}}=\frac{S_{\mathrm{valve}}^{\mathrm{hyb}}}{S_{\mathrm{valve}}^{\mathrm{MMC}}} \tag{2}$$

where $S_{\mathrm{norm}}^{\mathrm{hyb}}$ is the normalized combined power rating of the hybrid converter in p.u., $S_{\mathrm{valve}}^{\mathrm{hyb}}$ and $S_{\mathrm{valve}}^{\mathrm{MMC}}$ the combined power rating in VA of the hybrid converter and the FB-MMC, respectively, both of which are calculated by (1), while $S_{\mathrm{o}}^{\mathrm{hyb}}$ and $S_{\mathrm{o}}^{\mathrm{MMC}}$ is the transferred power by the hybrid converter and the MMC, respectively. Therefore, the ratios $S_{\mathrm{valve}}^{\mathrm{hyb}}/S_{\mathrm{o}}^{\mathrm{hyb}}$ and $S_{\mathrm{valve}}^{\mathrm{MMC}}/S_{\mathrm{o}}^{\mathrm{MMC}}$ represent the combined power rating per unit of transferred power of the hybrid converter and the MMC, respectively. Yet, as mentioned in the conditions for the comparison of the hybrid converters, the calculations of the combine power rating of semiconductors are performed for the same transferred power; hence, $S_{\mathrm{o}}^{\mathrm{hyb}}=S_{\mathrm{o}}^{\mathrm{MMC}}$ and both of these variables are eliminated in (2).

The power rating of the thyristor and the VSC valves of the hybrid converters presented in this article have been calculated based on the previously described method and are summarized in Table II. Table II shows that most of the hybrid converters have lower VSC valve rating compared to the FB-MMC, apart from the TBPG-MMC. The reason is that the peak current of this converter is higher than that of the FB-MMC, as it is assumed to operate as the EO-AAC and at $M=1$. The combined power rating of the thyristors is in the range of 0.5–0.7 p.u. for most of the hybrid converters except for the AFCB-MMC, the AAC, and the HACC. The first requires more thyristor rating because it is constructed by thyristor-based half-bridge SMs, the second requires less thyristor rating due to the reduced voltage rating of the director switches (when operated as the EO-AAC [16]) compared to the cluster of FB SMs per arm, the third required less thyristor rating due to the reduced peak current, while the third mainly comprises RC/RB switches.

The qualitative characteristics of the hybrid converters of Table II are outlined in Table III, which shows that the converters with the lowest conduction losses are the AFCB, the TBPG-MMC, the CTB, and the METDC. Moreover, most of the topologies do not suffer from ac/dc coupling due to their capability to control the modulation index in a wide range without adjusting the dc-side voltage. The exceptions are the CTB, the HACC, and the METDC. The CTB, which is the ECTB without the series decoupling circuits, operates in a narrow range of modulation indices; yet, modulation techniques have been developed for extending this range sufficiently for the HVdc applications [19]. The HACC should be operated in a narrow range of modulation indices for ensuring equal peak currents through all arms. Moreover, the METDC are limited to a narrow range of modulation indices because the peak ac-side voltage is linked to the dc-link voltage.

Most of the topologies feature good harmonic performance, meaning that they do not introduce lower order harmonics in the voltages/currents either on the ac or dc sides. The only exceptions are the AFCB-MMC, the CTB without the series decoupling circuits connected to the ac terminals, and the METDC. Another exception is the thyristor-based AAC that is not operated in the EO-AAC mode, which generates low-order current harmonics on the dc side [15].

By comparing Tables II and III, it can be observed that there is a tradeoff between the favorable VSC features and the total VSC rating. More specifically, the converters with low-VSC power rating, like the CTB and the AFCB, tend to lose favorable VSC features, like good harmonic performance and wide modulation index range. Thus, the low-VSC power rating seems to be an indication that the hybrid converters might have more similarities to the LCC rather than the VSC, in terms of steady-state operation. One exception to this is the MEMC that features the favorable VSC characteristics at low VSC power rating. On the other hand, the hybrid converters with higher VSC power rating and lower thyristor rating, such as the TBPG-MMC and the ECTB, seem to have more similarities to the VSC rather than the LCC.

B. Discussion on Fault-Ride-Through Capabilities

For HVdc applications, the converters are typically required to ride through the following faults:

1) dc-side faults, during which the dc-link voltage drops significantly (i.e., by more than 50%);
2) symmetric ac-side faults, during which the voltage of all three phases drops significantly (i.e., by more than 50%); and
3) asymmetric ac-side faults, during which the voltage of one or two phases drops significantly (i.e., by more than 50%).

Therefore, the capability of the hybrid converters to ride-through these faults is quite important. Yet, as the evaluation of fault-ride-through capability is a complex process that requires extensive simulation studies, the purpose of this section is to merely discuss the potential of the hybrid converters of Table III to ride-through the aforementioned faults.

The hybrid converters described in this article consist of FB-SM clusters and thyristors, which offer the possibility of handling dc faults in different ways. Some potential ways of dc-fault ride through are listed as follows.

1) DC-fault ride-through via the FB-SM clusters: this can be achieved by diverting the dc-fault current in conduction paths with FB SMs, which can inject voltages that oppose and extinguish the fault current or can operate in STATCOM mode.
2) DC-fault ride-through via LCC mode of thyristor bridges: this can be achieved by diverting the majority of the dc-fault current in the thyristor bridges and using a control strategy similar to that of an LCC (i.e., driving the converters at both sides of an HVdc link into inverter mode, as described in [1, Ch. 8]);
3) DC-fault ride-through via double thyristor bypass: this can be achieved by triggering thyristors in both directions, so that both dc and ac sides are short-circuited and isolated from each other, as shown in [42];
4) DC-fault ride-through via thyristor bypass and STATCOM (or blocking) mode of FB-SM clusters: this is performed by turning ON the suitable thyristors that both short-circuit the dc link (see previous point) and interconnect the FB-SM clusters in a configuration that can operate in STATCOM mode (or enter in the blocking state for inhibiting the ac-side to feed fault current to the dc side);
5) DC-fault ride-through via thyristor bypass/block: this is performed by turning ON the suitable thyristors for short-circuiting the dc link, combined by blocking other thyristors to interrupt the current path from the ac to the dc side.

However, note that these dc-fault ride-through strategies are not applicable to any hybrid converter of Table III. Notably, each hybrid converter might not be able to employ all these strategies, while the fifth strategy can only be utilized by the METDC. For example, the TBPG-MMC can ride through dc faults by utilizing the first strategy, as demonstrated in [31] and [32], or the second or third strategies, but not the fourth strategy; this is because thyristor bypassing would lead to bypassing of all FB-SM clusters and thus STATCOM mode of the latter is not possible. The first strategy can be utilized by the TBPG-MMC, the thyristor-based AAC, the ECTB, and the HACC. Furthermore, the second strategy can be employed by all hybrid converters of Table III except for the thyristor-based AAC and the MEMC; yet, it might not be the most preferred option for the ECTB and the HACC, as a portion of the thyristor-valve current necessarily flows through FB-SM clusters. The third dc-fault ride-through strategy can be utilized by the AFCB-MMC, the TBPG-MMC, and the CTB, while the fourth strategy can be utilized by the ECTB, the MEMC, the HACC. Finally, the METDC can utilize only the fifth strategy, as its mixed HB/FB-SM clusters are not in the fault-current path. In summary, all hybrid converters of Table III can handle dc faults by employing one or several of the outlined strategies.

Furthermore, the capability of the hybrid converters of Table III to ride through ac faults is linked to the modulation index range at which these converters can operate. Notably, the hybrid converters that can operate at a wide modulation index range have the potential to ride through both symmetric and asymmetric ac faults. However, a narrow modulation index range indicates that ac-fault ride-through will be challenging, if not impossible. More specifically, symmetric ac faults for which the voltage of all phases drops significantly (i.e., by more than 50%) would require tap-changing functionality for the converter transformers. In this way, the voltage at the converter winding of the transformer can be regulated to levels that are within the modulation index range of the converter.

Moreover, dealing with asymmetric ac faults might require to devise special strategies (control and/or modulation) for extending the modulation index range and operating with different per-phase modulation indices during the faults. This is because in asymmetric ac faults, the voltage of one or two phases drops significantly and hence the modulation index of the corresponding converter phase legs needs to be reduced accordingly; this reduction imposes modulation indices that are outside of the narrow range that can be utilized during steady-state conditions. In addition, the phase leg(s) that are connected to the healthy phase(s) must operate at modulation indices suitable to support the nominal grid voltage. One notable example of such a special strategy is the one developed for the CTB in [19]. In this case, the modulation index range is extended at the expense of deteriorated harmonic performance, which is an acceptable tradeoff during faults. Finally, note that, similarly to symmetric ac faults, per phase tap-changing control might be a possible option for allowing the hybrid converters with narrow modulation index range to ride through asymmetric ac faults.

VI. HVDC System Based on Hybrid Topologies

A. Hybrid LCC and VSC HVDC Converter Station Structures

It is clear from the previous sections and Table I that the thyristor-based LCC and IGBT-based MMC have complementary characteristics. It is highly desirable to have an HVdc system, which, preserves the combined advantages of a VSC and an LCC in one unit without suffering from their disadvantages. Recently, significant research interests have developed to form/derive hybrid HVdc converter stations by combining LCC

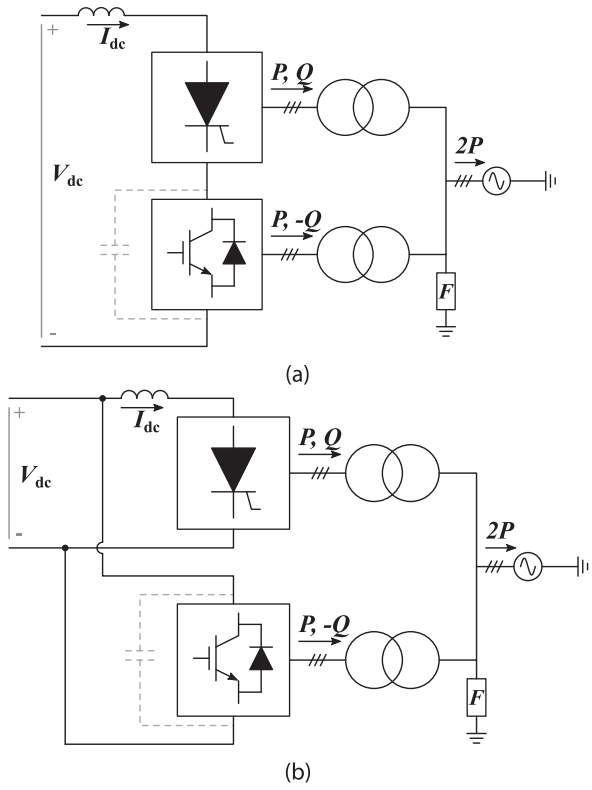

Fig. 10. Hybrid converter with LCC and MMC. (a) Series [48]–[52] and (b) parallel [53], [54] hybrid converter HVdc systems. Note that in high-power HVdc applications, single-phase transformers are typically employed. Active and reactive power flows are denoted by appropriate arrows and signs.

and MMC technologies. In all these hybrid configurations, the LCC and VSC are combined at the converter level without any significant changes in their operating principles and functionalities.

There are two broad categories of hybrid converter structures. The first category combines a VSC and an LCC by treating them as independent units (HVdc-station level) by connecting them in series at the dc side and in parallel at the same ac-side busbar. There are two possible configurations for such a hybrid converter system, the dc-series [48]–[52] and the dc-parallel [53], [54] one. More complicated structures by combining dc-series and dc-parallel configurations are also possible, but they require complicated control, more semiconductors, and higher costs; yet, such complicated structures may prove advantageous in certain applications, as discussed in [55]. Such hybrid dc-series and dc-parallel systems can offer benefits such as generation of the needed LCC reactive power by the VSC [48], [49], independent P-Q control [49], [56], interconnection to a weak ac system, lower risk of commutation failure using fast alternate-voltage control [49], [52], [57], [58], and reduction/elimination of the ac filters required for the LCC, provided that the VSC can be used as an active filter [50], [59], [60].

A dc-series hybrid converter consists of a series connection at the dc side of one LCC and one VSC, as shown in Fig. 10(a) [48]–[52]. In this configuration the VSC, while participating in active power transfer, also generates the reactive power demand of the LCC and supports the ac terminal voltage. This configuration may be considered for upgrading of an LCC connected to a weak ac power system. In such a case, where increasing the dc-link current is not an option, the inverter voltage may be increased by connecting a new VSC in series to the existing LCC. This series system also features the advantage that the VSC does not contribute any short-circuit power during a solid ac-side fault [53]. Hence, the short-circuit power capability of the grid can be low. However, one of the main limitations of this configuration is the complexity of the dynamic power reversal, which needs additional mechanical switches to interchange the dc pole connections for reversing the voltage polarity across the VSC [49], [53]. This is because the power reversal for the LCC is achieved by reversing the direct-voltage polarity by firing angle control, while the current direction remains unchanged [10], [49]. Nonetheless, if VSCs with voltage-reversal capability, such as the full-bridge MMC [56], are employed, the dynamic power reversal can be greatly simplified.

A dc-parallel hybrid converter, which can be considered as the dual form of the dc-series hybrid converter, consists of a parallel connection of one LCC and one VSC, as shown in Fig. 10(b) [53], [54]. This configuration can be considered for providing real power to a very weak electrical system, which is not possible with only LCC. It can also be used for power upgrading of an existing LCC system connected to a weak ac system. In such cases, it is required for generating reactive power [53]. Since the dc-link voltage cannot be increased, a new parallel VSC added to the LCC can help in increasing the inverter current. Since the VSC can also fulfil the reactive power demands of LCC, the static capacitor banks (see Fig. 2) may be eliminated. Note that the dc-parallel system may not be suitable for very high-voltage applications due to the rating limitations of IGBTs if the conventional two-level VSCs are used. Nonetheless, this limitation can be addressed up to some extent by using the MMC [9] as the parallel connected VSC. The dc-parallel hybrid system also suffers from the limitation of dynamic power reversal in the same way as the dc-series system. Again, this limitation is not applicable to the VSC topologies that have the capability to reverse their dc-link voltage, such as the FB-MMC [56].

In the second category of hybrid topologies, the LCC is used as the active-power-transmitting converter and the modular (or monolithic) VSC is used for reactive power compensation of the LCC. In these hybrid converters, the VSC can be connected to the ac terminals of the LCC either in series [61]–[63] or in parallel [64]–[67], as illustrated in Fig. 11(a) and (b). In [56], a detailed review and analysis of such topologies with modular VSCs is presented. The modular VSCs, constructed by FB SMs, inject voltage (when connected in series to the LCC ac terminals) or current (when connected in parallel to the LCC ac terminals) at the ac side of the LCC and can be realized using different circuit configurations, as shown in [56]. Finally, hybrid converters of both the first (LCC and VSC connected in series at the dc side and in parallel at the ac side) and the second (VSC connected in series or parallel at the ac terminals of the LCC) categories are compared in terms of semiconductor power rating and the capability to independently control the active and reactive powers in [56].

TABLE IV
COMPARISONS OF THE HYBRID STATIONS OF Fig. 10

	Series hybrid station [Fig. 10(a)]	Parallel hybrid station [Fig. 10(b)]
VSC dc-terminal voltage rating	Partial dc-link voltage	DC-link voltage
VSC dc-terminal current rating	DC-link current	Partial dc-link current
Active-power limitation	Limited by VSC current rating	Limited by LCC and VSC current rating
Voltage/current source	Current source	Voltage source
Suitable VSC topology	High-current capable VSC (e.g., HACC)	High-voltage capable VSC (e.g., Series hybrid MMC)

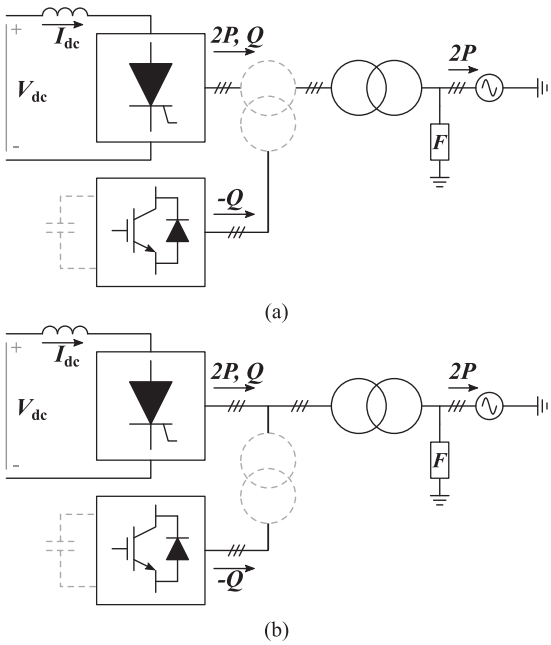

Fig. 11. Hybrid converters with the LCC transferring active power and the VSC compensating the reactive power of the LCC. The VSC can be connected to the ac terminals of the LCC in: (a) series [61]–[63]; or (b) parallel [64]–[67]. Note that the VSCs can be connected to the primary or secondary winding of the LCC transformers with or without VSC transformers. Active and reactive power flows are denoted by appropriate arrows and signs.

B. Comparisons of Hybrid Stations

Table IV shows the comparisons between series hybrid station and parallel hybrid station. Note that comparison is performed under the following conditions.

1) The LCC is in current control mode for the dc side.
2) The VSC can be either in voltage or current control mode for the dc side.
3) The ac- and dc-side systems are identical for both hybrid stations.
4) The turns ratio of all transformers is 1:1.

Since the stations are dual configuration of each other, the voltage and current rating of VSC converters are also dual relationship. The IGBT current limits a possible maximum active power transfer of the LCC for the series hybrid station, whereas the parallel hybrid station can utilize all power capability of the converters. The VSC can operate either voltage control mode or current control mode, where the LCC should operate opposite way from the VSC. Due to the constraint of current rating of the VSC, a suitable hybrid topology should be selected based on the station configuration, e.g., series hybrid station requires a high-current capable VSC to maximize the LCC power, whereas the parallel hybrid station requires high-voltage capable VSC to match with LCC rating.

Similar to the hybrid stations of Fig. 10, the two stations shown in Fig. 11 are also dual. Notably, the VSC of the hybrid station shown in Fig. 11(a) and (b) can provide reactive power by injecting voltage and current, respectively, to the ac-side of the LCC. The power rating of the VSCs is defined by the level of reactive power compensation required, while the dc-link voltage can be decided based on the turns ratio of the employed transformers, which is an important degree of freedom on the design of these VSCs. For example, a VSC with the same voltage and current rating could be used as either the series VSC of Fig. 11(a) or the parallel VSC of Fig. 11(b), if a transformer that either steps downs or steps up the VSC voltage is employed, respectively.

Furthermore, a common dc link for both the series and parallel VSCs is desirable for allowing energy exchange between the different phases of the VSCs. This is important for compensating the negative sequence voltage/current together with positive sequence voltage/current without significant converter overdimensioning, as observed in modular STATCOMs [68], [69]. Suitable hybrid topologies for the series and parallel VSCs of Fig. 10 are those that can achieve high reactive-power capability with minimum semiconductor power rating.

VII. CONCLUSION

This article presents the derivation, evaluation, and topology selection methodologies of hybrid converters comprising of IGBTs and thyristors. These hybrid converters combine significant benefits of both the LCC and VSC technologies. Various topologies are developed using different combinations of RB or RC switches and clusters comprising of VSC SMs. The proposed method for deriving hybrid converters is based on the topology tree that is introduced in this article. By using the

proposed derivation method, different hybrid converters have been synthesized and categorized. A detailed comparison of several hybrid converters based on some important criteria, such as efficiency, modulation index range, harmonic profiles on ac/dc sides, and semiconductor power rating, is presented. This comparison shows that the behavior of hybrid converters can be more similar to either the LCC or the VSC, depending on the ratio of thyristors and IGBTs employed. Several hybrid LCC and VSC HVdc converter station configurations are analyzed and compared. In most cases, the specific application requirements dictate the most suitable hybrid converter configuration. General trends, challenges, and future scopes in the field of hybrid converter technology are presented as well. Active and continuous research in this area is important to provide the best candidate that could replace both the LCC and MMC technologies without losing the functionality required for the HVdc systems. It is clear that new grid codes, new application requirements, and the development of semiconductor devices will drive the future research in this area.

REFERENCES

[1] J. Arrillaga, High Voltage Direct Current Transmission, IET Power and Energy Series 29, 2nd ed. London, U.K: IET, 1998.

[2] B. Jacobson, Y. Jiang-Häfner, P. Rey, and G. Asplund, "HVDC with voltage source converters and extruded cables for up to ± 300 kV and 1000 MW," in *Proc. CIGRE*, 2006.

[3] N. Flourentzou, V. G. Agelidis, and G. D. Demetriades, "VSC-based HVDC power transmission systems: An overview," *IEEE Trans. Power Electron.*, vol. 24, no. 3, pp. 592–602, Mar. 2009.

[4] E. Spahic, F. Schettler, D. Varma, and J. Dorn, "Impact of the dc technology on transmission grids," in *Proc. 11th IET Int. Conf. AC DC Power Transmiss.*, 2015, pp. 1–7.

[5] G. Li *et al.*, "Feasibility and reliability analysis of LCC dc grids and LCC/VSC hybrid dc grids," *IEEE Access*, vol. 7, pp. 22 445–22 456, Feb. 2019.

[6] ABB, "HVDC classic–Thyristor valve projects," 2017. [Online.] Available: https://new.abb.com/systems/hvdc/hvdc-classic. [Accessed: Apr 16, 2019].

[7] ABB, "HVDC light–It's time to connect," 2017. [Online.] Available: https://new.abb.com/systems/hvdc/hvdc-light. Accessed: Apr 16, 2019.

[8] A. Nami, J. Liang, F. Dijkhuizen, and G. D. Demetriades, "Modular multilevel converters for HVDC applications: Review on converter cells and functionalities," *IEEE Trans. Power Electron.*, vol. 30, no. 1, pp. 18–36, Jan. 2015.

[9] A. Lesnicar and R. Marquardt, "An innovative modular multilevel converter topology suitable for a wide power range," in *Proc. IEEE Bologna Power Tech Conf. Proc.*, Jun. 2003, pp. 1–6.

[10] J. Arrillaga, Y. H. Liu, and N. R. Watson, *Flexible Power Transmission: The HVDC Options*. Hoboken, NJ, USA: Wiley, 2007.

[11] D. R. Trainer, W. Crookes, T. C. Green, and M. M. C. Merlin, "HVDC converter comprising fullbridge cells for handling a dc side short circuit," Eur. Patent EP 2 599 199 B1, Jul. 30, 2010.

[12] M. Merlin *et al.*, "A new hybrid multi-level voltage-source converter with DC fault blocking capability," in *Proc. 9th IET Int. Conf. AC DC Power Transmiss.*, Oct. 2010, pp. 1–5.

[13] D. R. Trainer *et al.*, "A new hybrid voltage-sourced converter for HVDC power transmission," in *Proc. CIGRE*, 2010.

[14] C. C. Davidson, A. C. Lancaster, A. J. Totterdell, and C. D. M. Oates, "A 24 MW level voltage source converter demonstrator to evaluate different converter topologies," in *Proc. CIGRE*, 2012.

[15] M. M. C. Merlin *et al.*, "The alternate arm converter: A new hybrid multilevel converter with DC-fault blocking capability," *IEEE Trans. Power Del.*, vol. 29, no. 1, pp. 310–317, Feb. 2014.

[16] M. M. C. Merlin *et al.*, "The extended overlap alternate arm converter: A voltage-source converter with DC fault ride-through capability and a compact design," *IEEE Trans. Power Electron.*, vol. 33, no. 5, pp. 3898–3910, May 2018.

[17] D. Soto-Sánchez, M. Martínez-Gómez, I. Andrade, and R. Peña, "Alternate arm converter with thyristor-based director switches," in *Proc. IEEE Int. Conf. Autom./XXIII Congr. Chilean Assoc. Autom. Control*, Oct. 2018.

[18] D. C. Trainer, R. W. Crookes, and C. Oates, "Converter," Worldwide Patent WO2 011 050 847A1, May 5, 2011.

[19] C. Oates, K. Dyke, and D. Trainer, "The use of trapezoid waveforms within converters for HVdc," in *Proc. 16th Eur. Conf. Power Electron. Appl.*, Aug. 2014, pp. 1–10.

[20] C. Oates and K. Dyke, "The controlled transition bridge," in *Proc. 17th Eur. Conf. Power Electron. Appl.*, 2015, pp. 1–10.

[21] D. Zhang, L. J. Garces, R. Datta, and R. N. Raju, "Multilevel power converter system and method," U.S. Patent US 2014/0 092 661 A1, Apr. 3, 2014.

[22] D. Zhang, R. Datta, A. Rockhill, Q. Lei, and L. Garces, "The modular embedded multilevel converter: A voltage source converter with IGBTs and thyristors," in *Proc. IEEE Energy Convers. Congr. Expo.*, Sep. 2016, pp. 1–8.

[23] D. Zhang, D. Dong, R. Datta, A. Rockhill, Q. Lei, and L. Garces, "Modular embedded multilevel converter for MV/HVDC applications," *IEEE Trans. Ind. Appl.*, vol. 54, no. 6, pp. 6320–6331, Nov. 2018.

[24] S. K. Patro and A. Shukla, "Highly efficient fault-tolerant modular embedded thyristor directed converter for HVdc applications," *IEEE Trans. Power Del.*, vol. 35, no. 1, pp. 349–363, Feb. 2020.

[25] R. Feldman, M. Tomasini, J. C. Clare, P. Wheeler, D. R. Trainer, and R. S. Whitehouse, "A low loss modular multilevel voltage source converter for HVDC power transmission and reactive power compensation," in *Proc. 9th IET Int. Conf. AC DC Power Transmiss.*, 2010, pp. 1–5.

[26] R. Feldman, *et al.*"A hybrid modular multilevel voltage source converter for HVdc power transmission," *IEEE Trans. Ind. Appl.*, vol. 49, no. 4, pp. 1577–1588, Jul. 2013.

[27] ABB, "Phase Control Thyristor–5STP 37Y8500," Jan. 2015, [Online.] Available: https://new.abb.com/semiconductors/thyristors/phase-controlled-pct. [Accessed: Apr. 16, 2019].

[28] ABB, "StakPak IGBT–5SMA 3000L450300," 2018. [Online.] Available: https://new.abb.com/semiconductors/stakpak. Accessed: Apr. 16, 2019.

[29] P. Li, S. J. Finney, and D. Holliday, "Thyristor based modular multilevel converter with active full-bridge chain-link for forced commutation," in *Proc. IEEE 17th Workshop Control Model. Power Electron.*, Jun. 2016, pp. 1–6.

[30] P. Li, S. J. Finney, and D. Holliday, "Active-forced-commutated bridge using hybrid devices for high efficiency voltage source converters," *IEEE Trans. Power Electron.*, vol. 32, no. 4, pp. 2485–2489, Apr. 2017.

[31] P. D. Judge, M. C. Merlin, T. C. Green, D. R. Trainer, and K. Vershinin, "The augmented trapezoidal alternate arm converter: A power-group augmented DC fault tolerant voltage source converter," in *Proc. 2nd Int. Conf. High Voltage Direct Current*, Oct. 2016, pp. 1–6.

[32] P. D. Judge, M. M. Merlin, T. C. Green, D. R. Trainer, and K. Vershinin, "Thyristor-bypassed submodule power-groups for achieving high-efficiency, DC fault tolerant multilevel VSCs," *IEEE Trans. Power Del.*, vol. 33, no. 1, pp. 349–359, Feb. 2018.

[33] P. D. Judge, M. M. Merlin, T. C. Green, D. R. Trainer, and K. Vershinin, "Thyristor/diode-bypassed submodule power groups for improved efficiency in modular multilevel converters," *IEEE Trans. Power Del.*, vol. 34, no. 1, pp. 84–94, Feb. 2019.

[34] P. Briff, R. Ginnareddy, S. Dang, O. Idehen, K. Vershinin, and D. Trainer, "The controlled transition bridge: Analysis and benchmarking for the HVDC VSC market," in *Proc. 20th Eur. Conf. Power Electron. Appl.*, Sep. 2018, pp. P.1–P.8.

[35] P. Bakas, K. Ilves, S. Norrga, L. Harnefors, and H.-P. Nee, "Hybrid alternate-common-arm converter with director thyristors—Impact of commutation time on the active-power capability," in *Proc. 21st Eur. Conf. Power Electron. Appl.*, Sep. 2019, pp. 1–11.

[36] P. K. Barupati, T. Jonsson, and S. Subramanian, "Thyristor based voltage source converter," Eur. Patent EP 2 926 449 B1, Nov. 27, 2012.

[37] A. Nami, K. Ilves, and M. Rahimo, "A hybrid modular multilevel converter," Swedish Patent SE 1 551 618 A1, Dec. 10, 2015.

[38] K. Ilves, L. Harnefors, and P. Bakas, "Submodule for a modular multilevel converter," Worldwide Patent WO 2 019 007 475 A1, Jul. 3, 2017.

[39] F. J. Moreno and D. R. Trainer, "Hybrid modular multicell converter with bidirectional thyristor switches," Eur. Patent EP 2 999 105 A1, Sep. 17, 2014.

[40] D. C. Davidson, I. B. Efika, and D. C. Trainer, "Semiconductor switching circuit," U.S. Patent US20 170 126 015A1, May 4, 2017.

[41] Y. A. Rudrasimha, M. B. Ghat, and A. Shukla, "A new hybrid submodule for MMC with DC fault ride-through capability," in *Proc. IEEE Int. Conf. Power Electron., Drives Energy Syst. Conf.*, Dec. 2018, pp. 1–6.
[42] X. Li, Q. Song, W. Liu, H. Rao, S. Xu, and L. Li, "Protection of nonpermanent faults on DC overhead lines in MMC-based HVDC systems," *IEEE Trans. Power Del.*, vol. 28, no. 1, pp. 483–490, Jan. 2013.
[43] B. Odegard, D. Weiss, T. Wikstrom, and R. Baumann, "Rugged MMC converter cell for high power applications," in *Proc. 18th Eur. Conf. Power Electron. Appl.*, Sep. 2016, pp. 1–10.
[44] U. Pengfei H., J. Daozhuo, G. Jie, Z. Yuebin, and L. Yiqiao, "Hybrid multilevel converters based on thyristor alternate-arms," *Autom. Elect. Power Syst.*, vol. 36, pp. 102–107, 2012.
[45] P. Bakas, K. Ilves, L. Harnefors, S. Norrga, and H.-P. Nee, "Hybrid converter with alternate common arm and director thyristors for high-power capability," in *Proc. 20th Eur. Conf. Power Electron. Appl.*, Sep. 2018, pp. 1–10.
[46] A. Darwish, "Efficient modular multilevel converter based on active-forced-commutated hybrid packed u-cells for HV networks," in *Proc. 15th IET Int. Conf. AC DC Power Transmiss.*, 2019, pp. 1–6.
[47] Q. Wang, F. Deng, C. Liu, Q. Heng, and Z. Chen, "Thyristor-based modular multilevel converter-HVDC systems with current interruption capability," *IET Power Electron.*, vol. 12, no. 12, pp. 3056–3067, Oct. 2019.
[48] B. Qahraman and A. Gole, "A VSC based series hybrid converter for HVDC transmission," in *Proc. Can. Conf. Elect. Comput. Eng.*, May 2005, pp. 458–461.
[49] G. Andersson and M. Hyttinen, "Skagerrak: The next generation," in *Proc. CIGRE Symp.*, 2015.
[50] H. Jiang and Å. Ekström, "Harmonic cancellation of a hybrid converter," *IEEE Trans. Power Del.*, vol. 13, no. 4, pp. 1291–1296, Oct. 1998.
[51] D. Trainer, A. P. Canelhas, C. C. Davidson, and C. D. Barker, "Hybrid HVDC converter," Worldwide Patent WO 2011/124 258 A1, Apr. 8, 2010.
[52] W. Lin *et al.*, "Series VSC-LCC converter with self-commutating and dc fault blocking capabilities," in *Proc. IEEE PES Gen. Meeting, Conf. Expo.*, Jul. 2014, pp. 1–5.
[53] B. Qahraman, "Series/Parallel Hybrid VSC-LCC for HVdc Transmission Systems," Ph.D. dissertation, Univ. Manitoba, Winnipeg, Canada, 2010.
[54] F. Fein and B. Orlik, "Dual HVDC system with line- and self-commutated converters for grid connection of offshore wind farms," in *Proc. Int. Conf. Renew. Energy Res. Appl.*, Oct. 2013, pp. 280–285.
[55] W. Xiang, *et al.*, "A cascaded converter interfacing long distance hvdc and back-to-back hvdc systems," *IEEE J. Emerg. Sel. Topics Power Electron.*, to be published, doi: 10.1109/JESTPE.2019.2913915.
[56] P. Bakas *et al.*, "A review of hybrid topologies combining line-commutated and cascaded full-bridge converters," *IEEE Trans. Power Electron.*, vol. 32, no. 10, pp. 7435–7448, Oct. 2017.
[57] H. Liu, X. Ni, C. Guo, Y. Liu, and C. Zhao, "Enhanced line commutated converter with embedded fully controlled sub-modules to mitigate commutation failures in high voltage direct current systems," *IET Power Electron.*, vol. 9, no. 2, pp. 198–206, Feb. 2016.
[58] Z. Xu, S. Wang, and H. Xiao, "Hybrid high-voltage direct current topology with line commutated converter and modular multilevel converter in series connection suitable for bulk power overhead line transmission," *IET Power Electron.*, vol. 9, no. 12, pp. 2307–2317, Oct. 2016.
[59] P. Briff, C. Udalagama, and K. Vershinin, "Filterless line commutated converter for HVDC transmission," in *Proc. 15th IET Int. Conf. AC DC Power Transmiss.*, Feb. 2019, pp. 1–6.
[60] P. Bakas *et al.*, "Design considerations and comparison of hybrid line-commutated and cascaded full-bridge converters with reactive-power compensation and active filtering capabilities," in *Proc. 21st Eur. Conf. Power Electron. Appl.*, Sep. 2019, pp. 1–13.
[61] T. Tanaka, M. Nakazato, and S. Funabiki, "A new approach to the capacitor-commutated converter for HVDC-a combined commutation-capacitor of active and passive capacitors," in *Proc. IEEE Power Eng. Soc. Winter Meeting Conf. Proc. (Cat. No. 01CH37194)*, vol. 2, pp. 968–973, 2001.
[62] M. Jafar and M. Molinas, "A transformerless series reactive/harmonic compensator for line-commutated HVDC for grid integration of offshore wind power," *IEEE Trans. Ind. Electron.*, vol. 60, no. 6, pp. 2410–2419, Jun. 2013.
[63] Y. Xue, X.-P. Zhang, and C. Yang, "Elimination of commutation failures of LCC HVDC system with controllable capacitors," *IEEE Trans. Power Syst.*, vol. 31, no. 4, pp. 3289–3299, Jul. 2016.
[64] B. Andersen and L. Xu, "Hybrid HVDC system for power transmission to island networks," *IEEE Trans. Power Del.*, vol. 19, no. 4, pp. 1884–1890, Oct. 2004.
[65] P. Fischer de Toledo, "Modelling and control of a line-commutated HVDC transmission system interacting with a VSC STATCOM," Ph.D. dissertation, KTH Royal Inst. Technol., Stockholm, Sweden, 2007.
[66] S. Bozhko, R. Blasko-Gimenez, R. Li, J. Clare, and G. Asher, "Control of offshore DFIG-based wind farm grid with line-commutated HVDC connection," in *Proc. 12th Int. Power Electron. Motion Control Conf.*, 2006, pp. 1563–1568.
[67] H. Zhou, G. Yang, and J. Wang, "Modeling, analysis, and control for the rectifier of hybrid HVDC systems for DFIG-based wind farms," *IEEE Trans. Energy Convers.*, vol. 26, no. 1, pp. 340–353, Mar. 2011.
[68] E. Behrouzian and M. Bongiorno, "Investigation of negative-sequence injection capability of cascaded H-bridge converters in star and delta configuration," *IEEE Trans. Power Electron.*, vol. 32, no. 2, pp. 1675–1683, Feb. 2017.
[69] E. Behrouzian, M. Bongiorno, J. R. Svensson, and A. Mohanaveeramani, "A proposed capacitor voltage-balancing strategy for double-Y STATCOM operated under unbalanced conditions," in *Proc. IEEE Energy Convers. Congr. Expo.*, Sep. 2019, pp. 998–1005.

Panagiotis Bakas (Member, IEEE) was born in Athens, Greece in 1984. He received the Diploma degree in electrical and computer engineering from the DUTH Democritus University of Thrace, Xanthi, Greece, in 2008, and the Ph.D. degree from the KTH Royal Institute of Technology, Stockholm, Sweden, in 2020.

Since July 2019, he has been with ABB Power Grids Research, Västerås, Sweden. His research interests include circuit design, modeling, modulation, and control of power-electronics converters for medium and high-power applications.

Yuhei Okazaki (Member, IEEE) was born in Kochi, Japan, in 1990. He received the B.S. degree from Kochi National College of Technology, Kochi, Japan, in 2012, and the M.Sc. and Ph.D. degrees from Tokyo Institute of Technology, Tokyo, Japan, in 2014 and 2017, respectively.

Since 2017, he has been working with ABB Power Grids Research, Sweden. His research interests include power-electronics converter topology, modeling, and control. He has authored/coauthored six IEEE transaction papers and totally ten issued and pending patents.

Anshuman Shukla (Senior Member, IEEE) received the M.Tech. and Ph.D. degrees in electrical engineering from the Indian Institute of Technology Kanpur, Kanpur, India, in 2003 and 2008, respectively.

From 2008 to 2011, he was a Scientist with ABB Corporate Research Center, Västerås, Sweden. In 2008, he was a Research Associate with the Department of Electrical Engineering, University of South Carolina, Columbia, SC, USA. He joined the Indian Institute of Technology Bombay, Mumbai, India, in 2011, where he is currently an Associate Professor with the Department of Electrical Engineering. His research interests include multilevel converters, power electronics for HVdc and FACTS applications, grid-connected renewable energy systems, solid state transformers, hybrid and solid-state circuit breakers, motor drives and the application of SiC power electronics.

Dr. Shukla was the recipient of the 2011 Young Engineer Award conferred by the Institution of Engineers, India. He is also the recipient of the MeitY Visveswaraya Young Faculty Research Fellowship 2018–2023. He is an Associate Editor for the IEEE JOURNAL OF EMERGING AND SELECTED TOPICS IN POWER ELECTRONICS.

Siba Kumar Patro (Student Member, IEEE) received the B.Tech. degree in electrical engineering from the Veer Surendra Sai University of Technology, Burla, India, in 2014. He is currently working toward the M.Tech.–Ph.D. dual degrees in electrical engineering from the Indian Institute of Technology Bombay, Mumbai, India.

In 2017, he joined the Visvesvaraya National Institute of Technology (VNIT), Nagpur, India, where he is currently working as a Trainee Teacher with the Department of Electrical Engineering. His research interests include power electronic converters for HVdc and FACTS applications, grid integration of renewable energy sources, and multilevel converters.

Kalle Ilves (Member, IEEE) received the M.Sc., Licentiate, and Ph.D. degrees in electrical engineering from the KTH Royal Institute of Technology, Stockholm, Sweden, in 2009, 2012, and 2014, respectively.

He joined the power-electronics team at ABB Corporate Research, Västerås, Sweden, in 2014. Since November 2019, he has been with the power-electronics team at ABB Power Grids Research in Västerås, Sweden. His research interests include modeling, control, modulation, and main-circuit design of high-power converters.

Frans Dijkhuizen (Member, IEEE) received the B.E. and Ph.D. degrees in electrical engineering from the Eindhoven University of Technology TU/e, Eindhoven, The Netherlands, in 1995 and 2003, respectively.

He joined ABB Corporate Research in Västerås Sweden, in 2001, working mainly in the field of high-power electronics. He is currently with ABB Power Grids Research for the ABB Power Grids Division, that will merge with Hitachi in July 2020. Since 2001, his areas of research include grid-connected power-electronics converters R&D for HVDC, FACTS, BESS, and active filter systems. He is a Senior Principal Scientist, inventor or co-inventor of 40+ patents, Affiliated Faculty with the University KTH,

Dr. Dijkhuizen is a member of the IEC/TC115/WG15 HVDC Grids Systems, and a frequent reviewer for the IEEE Power Electronics Society.

Alireza Nami (Senior Member, IEEE) received the Ph.D. degree in power electronics from Queensland University of Technology, Brisbane, Australia, in 2010.

From 2010 to 2011, he was a Postdoctoral Research Fellow in Global Center of Excellence, Kumamoto University, Japan. Since 2011, he has been with ABB Corporate Research Sweden and took several roles as a Principal Scientist in the area of high-power converter systems and control, R&D Project Leader, and the R&D Manager for the power-electronics team. He is currently a Research Center Manager for Power Grids Research in Sweden, which is a leading research group in high-power grid-connected products. He has served several leading power-electronics conferences as an invited speaker for industrial sessions and workshops, and a technical chair. He is the author/co-author of a number of IEEE conference and journal publications. He is inventor/co-inventor of several patent applications which have been adopted by the industry.

Dr. Nami is an Associate Editor of the IEEE TRANSACTION ON POWER ELECTRONICS, a member of CIGRE working groups, and a member of the International Scientific Committee of the European Power Electronics and Drives Association.